JOURNAL OF THERMOPHYSICS AND HEAT TRANSFER
Vol. 8, No. 2, April–June 1994

# Power-Law Fluid Flow in Heated Vertical Ducts

A. T. Jones* and D. B. Ingham†
*University of Leeds, Leeds, West Yorkshire LS2 9JT, England, United Kingdom*

**A hydrodynamically and thermally fully developed flow in a vertical duct is investigated. It is assumed that the wall of the duct is maintained at a temperature which varies linearly with respect to the depth of the duct to model a vertical duct in the Earth. Furthermore, in order to investigate flows during the drilling of muds and the cementing process in oil wells, the fluid is assumed to be a power-law fluid and the fluid flow in concentric annuli are investigated. The conditions under which multiple solutions are obtained is studied and the effects of the Rayleigh number $n$, the relative thickness of the channels, and the enforced pressure gradient are investigated.**

## Nomenclature

$d$ = half-width of duct
$k$ = thermal conductivity
$Nu$ = Nusselt number, Eq. (29)
$n$ = power-law index
$p$ = fluid pressure
$Ra$ = Rayleigh number, Eq. (8)
$T$ = temperature
$X, Y$ = nondimensional horizontal and vertical coordinates, Eq. (5)
$x, y$ = horizontal and vertical coordinates
$U, V$ = nondimensional horizontal and vertical velocities, Eq. (5)
$u, v$ = horizontal and vertical velocities
$\beta$ = coefficient of thermal expansion
$\dot{\gamma}$ = rate of strain tensor
$\delta_1, \delta_2$ = nondimensional thickness of duct wall and outer duct
$\zeta$ = nondimensional pressure gradient, Eq. (7)
$\Theta$ = nondimensional buoyancy, Eq. (5)
$\theta$ = temperature difference, $T - T_w$
$\lambda$ = applied temperature gradient
$\mu$ = coefficient of viscosity
$\rho$ = density of fluid

*Subscripts*
$D$ = duct region
$I$ = inner duct region
$n$ = quantities evaluated with $n$
$O$ = outer duct region
$W$ = wall region
$w$ = on outer wall of duct
$0$ = quantities evaluated at $T_0$

## Introduction

LAMINAR combined convection in vertical ducts, pipes, and annuli have become increasingly more important and have been studied, both analytically and numerically, by several authors. Until recently, these studies were largely restricted to forced convection flows and extensive literature surveys of this field have been performed.[1] However, in practice, many problems involving heat transfer in nuclear reactor flows, food production, the cooling of circuit cards, etc., are such that free convection affects are very important. In the specific case when a linear temperature gradient is applied to a thermally and hydrodynamically fully developed Newtonian flow, and the Boussinesq approximation has been made, then the resulting equations reduce to a fourth-order linear ordinary differential equation for which an analytical solution can be found. The original analysis for hydrodynamically fully developed flows by Ostrach[2] considered parallel plate ducts, whereas Morton,[3] Jackson et al.,[4] and Hanratty et al.[5] extended the study to circular pipes and Sherwin[6] and Maitra and Subba Raju[7] have investigated flows in annular regions.

The characteristic behavior of the solutions depends on the direction of the heating. When the wall temperature decreases with height, the buoyancy force aids the flow, and therefore increases the velocity everywhere. As the free convection effects increase, then the velocity increases rapidly until at a critical $Ra$ the velocity becomes infinite. This phenomena is known as "thermal runaway." This effect occurs first when $Ra = \pi^4/16$ and 33 in two-dimensional duct flow and circular pipe flow, respectively.[2,3,8] When the temperature on the outer wall increases with height, the opposing buoyancy and pressure forces reduce the velocity everywhere, and recirculation regions appear near the center for $Ra > 4\pi^4$ in a two-dimensional duct, and $Ra > 600$ in a circular pipe.

In the circulation of drilling muds and cement in the drilling, and cementing processes in oil wells, then the effect of buoyancy is very important, as is the thermal stratification of the earth and the non-Newtonian nature of the fluid. In order to keep the number of parameters to a minimum, we assume that the fluid may be adequately represented by a power-law fluid, although the Bingham-type fluid model is now more widely used. Furthermore, because in the Earth the temperature varies linearly with depth, we assume that the temperature of the outer wall of the duct varies linearly with distance along the duct. Also, in order to place cement in the region between the central piping (casing) and the rock face, the cement slurry is circulated down the casing and up the annular region between the case and the rock face. Since the ratio of the thickness of the annular region to the radius of the casing is usually very small, then the problem may be considered to be two-dimensional. Furthermore, the lengths of the casings are usually very long, and the Reynolds numbers are of moderate size, so that the flow over most of the length of the casing may be considered to be fully developed. Therefore, in this article we investigate both the fluid flow in three adjacent and parallel vertical two-dimensional ducts and the effects of the walls of the ducts having a finite thickness.

## Formulation of the Governing Equations

We assume that the Boussinesq approximation is valid, all physical properties are independent of the temperature, and

Received Nov. 17, 1992; revision received June 7, 1993; accepted for publication June 8, 1993. 

*Scientist, Department of Applied Mathematical Studies; currently at RR/56 Well Simulation, Shell, Rijswirk, Holland, L3-414.
†Professor, Department of Applied Mathematical Studies.

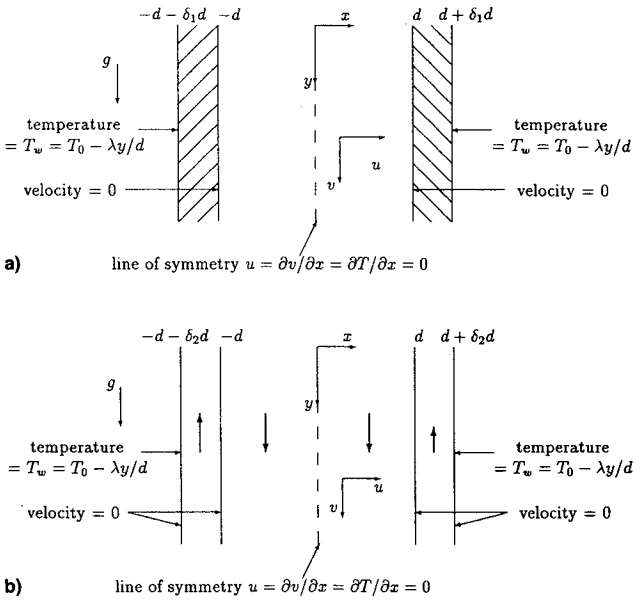


**Fig. 1 Flow geometries for cases a) I and b) II.**

viscous dissipation is ignored in accordance with Beckett.[8] Although real fluids exhibit large changes of viscosity with temperature, and smaller ones in diffusivity, these effects are secondary to the interaction of the buoyancy and pressure forces.

Two geometries are considered in this article (Fig. 1). The first, case I, corresponds to a two-dimensional vertical parallel plate duct of width $2d$ with a wall thickness $\delta_1 d$ (we will refer to case IA when $\delta_1 = 0$ and case IB when $\delta_1 \neq 0$), and the second, case II, is a counterflow in three adjacent channels, where the outer channel has width $\delta_2 d$. The circulating flow in case II is defined by the condition that the volume flux in the center duct is balanced by that in the outer two channels and is intended to provide a two-dimensional approximation of circulating cement around an oil well. The systems are referred to as two-dimensional Cartesian coordinates, with the $y$ axis vertically downwards and the origin on the centerline of the region. In each case a uniform temperature gradient $\lambda/d$ is applied in the vertical direction along the outer walls of the duct.

Consider the steady vertical flow of a power law fluid of density $\rho$ subject to a prescribed pressure gradient in either of the geometries shown in Fig. 1. We assume that the Boussinesq approximation is valid and the temperature of the outer wall is given by $T_w = T_0 - \lambda(y/d)$, where $T_0$ is the temperature of the wall measured at the level of the origin, and all the physical properties of the fluid are measured at $T_0$. For fluids with Prandtl numbers which are $\mathcal{O}(1)$, the velocity and buoyancy profiles develop over a distance which is $\mathcal{O}(Re\ d)$, and since the ratio of the length of the channels to the diameter are much greater than $Re$, then a hydrodynamically and thermally fully developed solution is sought where the velocity and buoyancy $(T - T_w)$ profiles are independent of the height $y$. If such a solution exists, then the temperature of the bulk of the fluid can be written as $T = T_w + \theta(x)$. The momentum equations are simplified by noting that the only nonzero components of $\underline{\dot{\gamma}}$ are $\dot{\gamma}_{xy} = \dot{\gamma}_{yx}$, where

$$\dot{\gamma}_{xy} = \dot{\gamma}_{yx} = \frac{\partial v}{\partial x} \tag{1}$$

Hence

$$(\underline{\nabla}\cdot\underline{\underline{\tau}})_x = -\frac{\partial(\eta\dot{\gamma}_{xy})}{\partial y} = 0 \tag{2}$$

$$(\underline{\nabla}\cdot\underline{\underline{\tau}})_y = -\frac{\partial(\eta\dot{\gamma}_{yx})}{\partial x} \tag{3}$$

and the vertical component of the full, steady momentum equations becomes

$$\frac{\mathrm{d}}{\mathrm{d}x}\left(\left|\frac{\mathrm{d}v}{\mathrm{d}x}\right|^{n-1}\frac{\mathrm{d}v}{\mathrm{d}x}\right) = \frac{\rho_0}{\mu_0}\left(\frac{1}{\rho_0}\frac{\mathrm{d}p}{\mathrm{d}y} - g\right) + \frac{\rho_0\beta g}{\mu_0}\theta \tag{4}$$

where $g$ is the acceleration due to gravity. It should be noted that the convective acceleration in Eq. (4) is identically zero since the flow is steady $\partial v/\partial y = 0$, and the horizontal component of the velocity is zero.

In order to assess the effects of the various parameters in the problem, Eq. (4) is nondimensionalized using the variables $X$, $V$, and $\Theta$, where

$$x = Xd, \qquad v = \alpha V/d, \qquad \theta = \lambda\Theta \tag{5}$$

and hence

$$\frac{\mathrm{d}}{\mathrm{d}X}\left(\left|\frac{\mathrm{d}V}{\mathrm{d}X}\right|^{n-1}\frac{\mathrm{d}V}{\mathrm{d}X}\right) = -\zeta_n + Ra_n\Theta \tag{6}$$

where

$$\zeta_n = -\frac{d^{2n+1}\rho_0}{\alpha^n\mu_0}\left(\frac{1}{\rho_0}\frac{\mathrm{d}p}{\mathrm{d}y} - g\right) \tag{7}$$

$$Ra_n = \frac{g\beta\lambda d^{2n+1}\rho_0}{\alpha^n\mu_0} \tag{8}$$

The nondimensional energy equation now reduces to

$$\frac{\mathrm{d}^2\Theta}{\mathrm{d}X^2} = -V \tag{9}$$

$\zeta_n$ and $Ra_n$ are functions of $n$, and if the values $Ra_n$ and $\zeta_n$ are prescribed, then the relative magnitudes of the pressure, viscous, and buoyancy forces are constant. In practice, both $\zeta_n$ and $Ra_n$ are $\mathcal{O}(1)$, but in some circumstances they may be as large as $\mathcal{O}(10^2)$. If the value of $n$ is allowed to vary, then this is not the same as fixing the values of $g\beta\lambda$ and $\mathrm{d}p/\mathrm{d}y$. Also, varying $Ra_n$ and $\zeta_n$ in the same proportion (i.e., $Ra_n \sim \zeta_n$), with the value of $n$ kept constant, is equivalent to varying the term $d^{2n+1}\rho_0/(\alpha^n\mu_0)$, which has the general form of a non-Newtonian Reynolds number.

For case IA, Eqs. (6) and (9) have to be solved subject to the nondimensional boundary conditions which are the symmetrical conditions

$$\frac{\mathrm{d}\Theta}{\mathrm{d}X} = \frac{\mathrm{d}V}{\mathrm{d}X} = 0 \qquad \text{on} \qquad X = 0 \tag{10}$$

and the specified temperature and no slip on $X = 1$

$$\Theta = V = 0 \qquad \text{on} \qquad X = 1 \tag{11}$$

where $\Theta(X) = (T - T_w)/\lambda$ has been employed.

In case IB, there is heat transfer in the wall region, and so Eqs. (6) and (9) have to be solved in the duct, and $\Theta$ varies linearly with $X$ in the wall. The symmetry condition is given by Eq. (10) and we have

$$\Theta_D = \Theta_W$$

$$k_D\frac{\mathrm{d}\Theta_D}{\mathrm{d}X} = k_W\frac{\mathrm{d}\Theta_W}{\mathrm{d}X} \tag{12}$$

$$V = 0 \qquad \text{on} \qquad X = 1$$

$$\Theta_W = 0 \qquad \text{on} \qquad X = 1 + \delta_1 \tag{13}$$

Using Eqs. (12) and (13), the nondimensional temperature in the wall can be written as

$$\Theta_W = \frac{k_D}{k_W}\frac{d\Theta_D}{dX}(X - 1 - \delta_1) \tag{14}$$

For case II, the conductivities of the fluid in the inner and outer regions are $k_I$ and $k_O$, respectively. The equations are nondimensional in terms of the properties of the inner region, and so Eqs. (6) and (9) hold for $0 \le X \le 1$, with all variables having the subscript $I$, and the governing equations in the outer region are given by

$$\frac{d}{dX}\left(\left|\frac{dV_O}{dX}\right|^{n-1}\frac{dV_O}{dX}\right) = \left(-\zeta_{n,0} + Ra_{n,0}\Theta_O\right)\frac{k_O}{k_I} \tag{15}$$

$$\frac{d^2\Theta_O}{dX^2} = -\frac{k_I}{k_O}V_O \tag{16}$$

The parameter $\zeta_I$ is assumed to be given, and the volume flux balance is used to evaluate $\zeta_O$ in terms of $\zeta_I$. The appropriate boundary condition on $X = 0$ is given by Eq. (10), with $V$ replaced by $V_I$ and the boundary condition (12) holds with $D$ and $W$ replaced by $I$ and $O$, respectively. Finally

$$\Theta_O = V_O = 0 \quad \text{on} \quad X = 1 + \delta_2 \tag{17}$$

and the conservation of volume flux gives

$$\int_0^1 V_I\,dX + \int_1^{1+\delta_2} V_O\,dX = 0 \tag{18}$$

## Forced Convection Solution

The limiting case of forced convection is studied in order to assess the effect of free convection on the flow and is given by substituting $Ra_n = 0$ in the appropriate equations. Hence, the solution of Eq. (6) is

$$V_I(X) = \frac{|\zeta_n|^{1/n-1}\zeta_n}{1/n + 1}(1 - |X|^{1/n+1}) \qquad 0 \le X \le 1 \tag{19}$$

In the outer regions of the adjacent channel case II, the velocity is given by

$$V_O(X) = C\left[\left(\frac{\delta_2}{2}\right)^{1/n+1} - \left|X - 1 - \frac{\delta_2}{2}\right|^{1/n+1}\right] \tag{20}$$

where

$$C = \frac{|\zeta_n|^{1/n-1}\zeta_n}{2(1/n + 1)}\left(\frac{2}{\delta_2}\right)^{1/n+2} \tag{21}$$

The buoyancy profiles, found by solving Eq. (9), are given by

$$\theta_I(X) = \frac{|\zeta_n|^{1/n-1}\zeta_n}{1/n + 1}\left[-\frac{X^2}{2} + \frac{|X|^{1/n+3}}{(1/n + 2)(1/n + 3)} + B_I\right] \qquad 0 \le X \le 1 \tag{22}$$

$$\Theta_O(X) = C\left[-\left(\frac{\delta_2}{2}\right)^{1/n+1}\frac{X^2}{2} + \frac{\left|X - 1 - \frac{\delta_2}{2}\right|^{1/n+3}}{(1/n + 2)(1/n + 3)} + A_O X + B_O\right] \qquad 1 \le X \le 1 + \delta_2 \tag{23}$$

where for case IA we have

$$B_I = \frac{1}{2} - \frac{1}{(1/n + 2)(1/n + 3)} = \frac{(1/n + 1)(1/n + 4)}{(1/n + 2)(1/n + 3)} \tag{24}$$

while in case II, we have

$$A_O = \left(\frac{\delta_2}{2}\right)^{1/n+1}\left[\frac{2/n + 3}{1/n + 2}\left(\frac{\delta_2}{2}\right) + 1\right] \tag{25}$$

$$B_O = -\frac{1}{2}\left(\frac{\delta_2}{2}\right)^{1/n+1} - \frac{2/n + 3}{1/n + 2}\left(\frac{\delta_2}{2}\right)^{1/n+2} - \left[\frac{2/n^2 + 8/n + 7}{(1/n + 2)(1/n + 3)}\right]\left(\frac{\delta_2}{2}\right)^{1/n+3} \tag{26}$$

$$B_I = \frac{(1/n + 1)}{(1/n + 2)}\left(\frac{1/n+4}{1/n + 3} - \frac{\delta_2}{2}\right) \tag{27}$$

## Results

Numerical solutions of Eqs. (6) and (9) have been obtained using a Runge Kutta Merson method subject to the boundary conditions (10) and (11) for case IA, (10), (12), and (13) for case IB, and (10), (12), (17), and (18) for case II. In all cases, results which are accurate to $\mathcal{O}(10^{-3})$ everywhere have been obtained. Typical computing times are of $\mathcal{O}(10)$ CPU s on an AMDAHL 5860 computer, when using a local convergence criterion for the velocity and buoyancy of less than $10^{-6}$.

Since the main aim of this article is to investigate the effects of counterflows in channels, then in this section only one example of the numerous situations considered is presented for case I. Figure 2 shows the velocity and buoyancy profiles in case IB for $\delta_1 k_D/k_W = 0.0$, 0.25, 0.5, and 0.75, with $Ra = -1.0$, $n = 0.5$, and $\zeta_{nI} = 1.0$. As $\delta_1 k_D/k_W \to 0$, the profiles tend towards those for the single duct in case IA, while as the value of $\delta_1 k_D/k_W$ increases, the magnitudes of the velocity and buoyancy force increase.

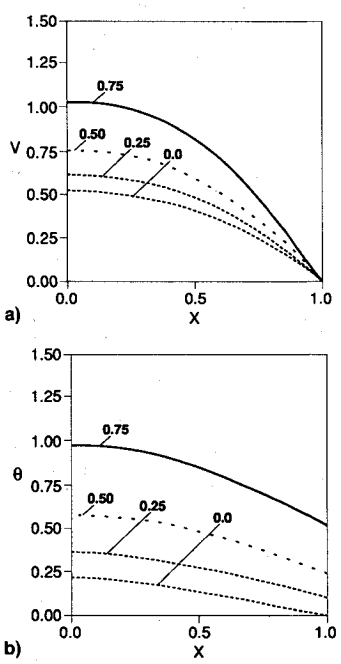


**Fig. 2 a) Velocity profile $V(X)$ and b) the buoyancy profile $\Theta(X)$ for case IB, with $n = 0.5$, $\zeta_{nI} = 1$, $Ra_n = -1.0$, and $\delta_1 k_D/k_W = 0.0$, 0.25, 0.5, and 0.75.**

For a geothermal gradient the temperature decreases with height, and for a Newtonian fluid, thermal runaway is predicted for $Ra < 0$. The velocity profile $V(X)$ and the buoyancy profile $\Theta(X)$ are shown in Fig. 3 for case II, with $Ra_n = \pm 1$, $\zeta_{nI} = 1$, $\delta_2 = 1$, and $n = 1.0$, 0.7, and 0.5. The situation when $n = 1$ corresponds to the Newtonian case. As $n \to 0.5$, the volume flux and buoyancy force increase (decrease) in the inner region $Ra = -1(+1)$, and there is a much greater increase in the velocity between $n = 0.7$ and $n = 0.5$ compared with that between $n = 0.9$ and $n = 0.7$ when $Ra = -1$. It can be seen that as the value of $n$ decreases, the shear rate near the walls increases (decreases) for $Ra = -1(+1)$, and the velocity profile near the center of each duct flattens. When the wall temperature decreases with height this differs from the forced convection solution in a single duct, where the velocity is proportional to $1 - |X|^{1/n+1}$ [Eq. (19)], and hence the shear-rate decreases over the entire width of the duct as the value of $n$ decreases.

Figure 4 shows the velocity and buoyancy profiles in case II for $n = 0.5$, $\delta_2 = 1$, and for various values of $Ra_n \sim \pm \zeta_{nI}$. As the values of $|Ra_n|$ and $\zeta_{nI}$ increase, the total volume flux and buoyancy force increase, since this is equivalent to increasing the non-Newtonian Reynolds number.

Figure 5 shows the change in the velocity and buoyancy profiles in case II for various values of $\delta_2$, and for $Ra_n = -1$, $\zeta_{nI} = 1$, and $n = 0.5$. As expected, the flow in the inner region decreases towards the solution in a single duct as the width of the outer channel decreases, and as the value of $\delta_2$ increases the magnitude of the peak velocity in the outer region decreases. It is observed that this decrease in peak velocity is more rapid than in the Newtonian case. This is due to the flattening of the velocity profile as the value of $\delta_2$ increases, which becomes more extreme as the value of $n$ decreases. Figure 5b shows that the buoyancy force increases as the value of $\delta_2$ increases.

Figure 6 shows the velocity and the buoyancy profiles for $Ra_n = 0.0$, $\pm 1.0$, and $\pm 2.0$, with $\zeta_{nI} = 1$, $n = 0.5$, and $\delta_2 = 1$, and varying the value of $Ra_n$ is equivalent to varying the buoyancy parameter $g\beta\lambda$. The forced convection solution is shown in Fig. 5 for comparison with the combined convection solution and corresponds to $Ra_n = 0$. As the value of $Ra_n$ increases, the magnitudes of the velocity and buoyancy force decrease over the entire duct as in the Newtonian case,

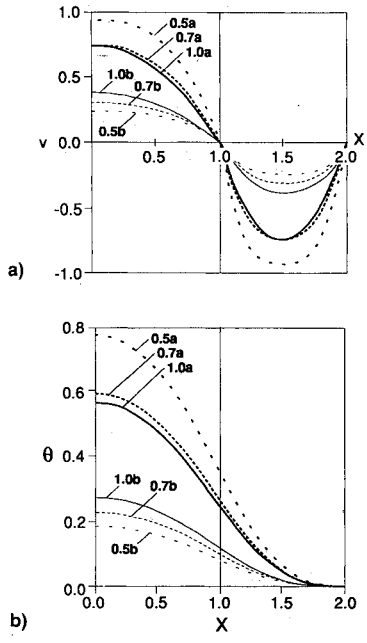


**Fig. 3 a) Velocity profile $V(X)$ and b) the buoyancy profile $\Theta(X)$ for case II, with $Ra_n = \pm 1$, $\zeta_{nI} = 1$, $\delta_2 = 1$, and $n = 0.5$, 0.7, and 1.0. *a* and *b* refer to − and + signs, respectively.**

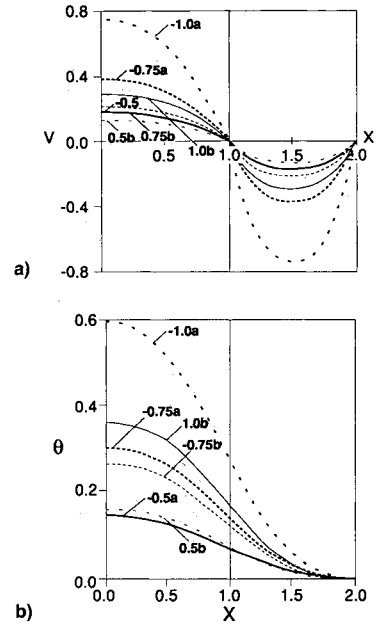


**Fig. 4 a) Velocity profile $V(X)$ and b) the buoyancy profile $\Theta(X)$ for case II, at various values of $Ra_n \sim \pm \zeta_{nI}$ with $n = 0.5$, $Ra_n/\zeta_{nI} = -1$, and $\delta_2 = 1$. *a* and *b* refer to − and + signs, respectively.**

but this increase becomes more rapid as the value of $n$ decreases.

## Heat Transfer Characteristics

The nondimensional mean temperature and Nusselt number are defined by

$$\bar{\Theta} = \int_0^1 \Theta \, dX \tag{28}$$

$$Nu = -\left(\frac{d\Theta}{dX}\right)_{X=1} \Big/ (\Theta - \Theta_w) \tag{29}$$

The forced convection Nusselt number for case IA is therefore given by

$$Nu = \frac{3(1/n + 4)}{1/n + 5} \tag{30}$$

and is unaffected by the presence of any outer region. Therefore, expression (30) gives the Nusselt number in the inner region for case II, and the forced convection Nusselt number in the outer region is given by

$$Nu_O = \frac{12(1/n + 4)}{4/n + 17} \tag{31}$$

In case II, the Nusselt numbers in the inner and outer regions are defined as

$$Nu_I = \left(\frac{\partial T_I}{\partial x}\right)_{x=d} d \Big/ \left[\frac{1}{d}\int_0^d T_I \, dx - (T_I)_{x=d}\right] \tag{32}$$

$$Nu_O = \left[\left(\frac{\partial T_0}{\partial x}\right)_{x=d} f_2 d\right] \Big/ \left[(T_0)_{x=d} - \frac{1}{\delta_2 d}\int_d^{d+\delta_2 d} T_0 \, dx\right] \tag{33}$$

Figure 7 shows the variation of the Nusselt numbers defined in Eqs. (32) and (33), as functions of $n$ with $Ra_n = -1$, $Ra_n = 0$, and $Ra_n = 1$. For the forced convection case, $Ra_n = 0$, Eqs. (30) and (31) imply that the values of $Nu_I$ and $Nu_O$ both

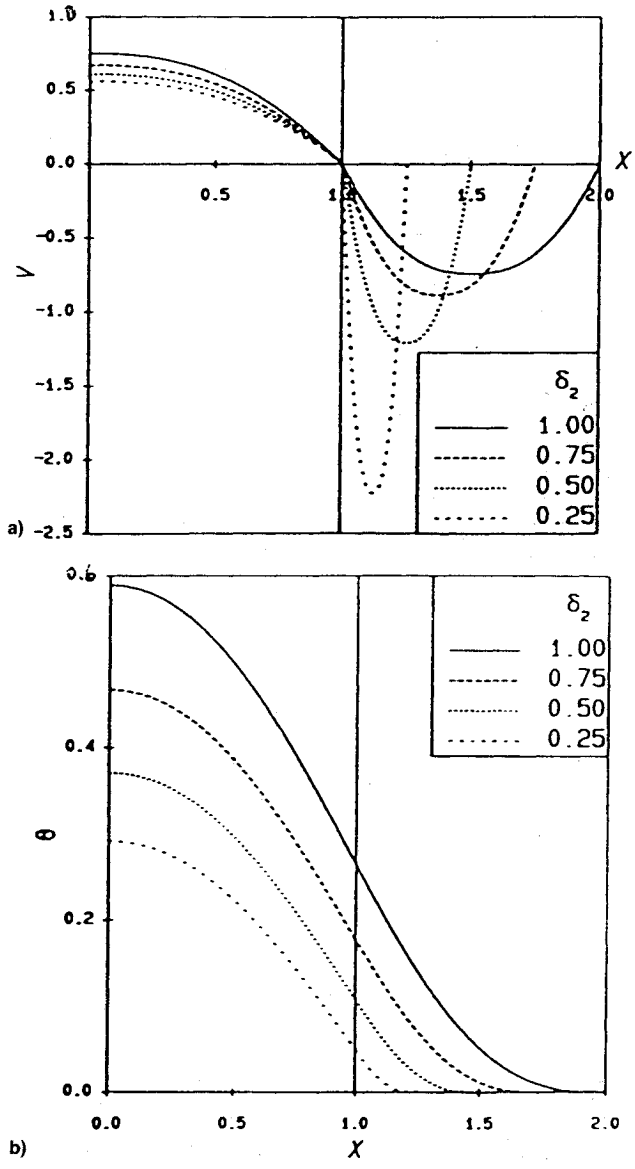


**Fig. 5 a) Velocity profile $V(X)$ and b) the buoyancy profile $\Theta(X)$ for case II, with $n = 0.5$, $Ra_n = -1$, $\zeta_{nl} = 1$ and $\delta_2 = 0.25, 0.5, 0.75$, and 1.0.**

tend to 3 as $n \to 0$, and as the value of $n$ increases towards the Newtonian case, $n = 1$, the values of $Nu_I$ and $Nu_O$ decrease towards 5/2 and 20/7, respectively. Hence, the decrease in the value of $Nu_I$ is more rapid than the decrease in the value of $Nu_O$, which varies little from the Newtonian value. The variations in $Nu_I$ and $Nu_O$ for $Ra_n \neq 0$ are similar to the forced convection case. However, for any given value of $n$, the values of the Nusselt numbers increase as the value of $Ra_n$ increases, and for the values of $Ra_n$ shown in Fig. 7 the greatest variation in the values of $Nu_I$ and $Nu_O$ with the value of $n$ occurs when $Ra_n = 1$.

## Multiple Solutions

The NAG routine D02HBF uses shooting methods, and so for the range of values of the parameters $Ra_n$ and $\zeta_{nl}$ where there are multiple solutions for the velocity, then different solutions can be obtained depending on the initial estimates made for the unknown parameters in the problem. For case I, Fig. 8 shows the variation of $V(0)$ as a function of $\log_{10}|Ra_n|$ for $Ra_n < 0$, and clearly there are multiple solutions. The various solutions, for the single duct, case I, can be found in the majority of regions defined by $|Ra_n| < 10{,}000$ by tracking the solution along one of the solution branches. To explain

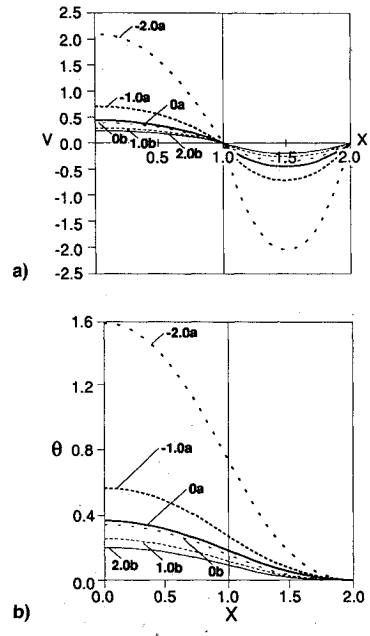


**Fig. 6 a) Velocity profile $V(X)$ and b) the buoyancy profile $\Theta(X)$, for case II, with $n = 0.5$, $\zeta_{nl} = 1$, $\delta_2 = 1$, and $Ra_n = 0.0, \pm 1.0$, and $\pm 2.0$. *a* and *b* refer to − and + signs, respectively.**

this further, the method for finding all the solutions over the range of Rayleigh numbers $|Ra_n| < 10{,}000$ is illustrated here.

To obtain solutions for the range of Rayleigh numbers $|Ra_n| < 1$, it has been found that a good initial estimate for the unknown parameters is not required. Therefore, the solution is first found for a value of $Ra_n$ in this range and is then tracked along curve (1), see Fig. 8, by gradually increasing the absolute value of the Rayleigh number. The solution for the previous value of $|Ra_n|$ is used to evaluate an approximation for the unknown parameters for the present value of $|Ra_n|$. Similar methods are applied to the other branches of the solution curves, except in the vicinity of the limit points, which are defined by

$$\frac{d|Ra_n|}{dV(0)} = 0 \quad \text{at} \quad Ra_n = Ra_c \tag{34}$$

Region A in Fig. 8 shows the neighborhood of one such limit point where there are three solution branches.

The shooting method becomes numerically unstable in some neighborhood of the limit points which is typically given by $|Ra_n - Ra_c| < \mathcal{O}(10)$. Due to the power-law nonlinearity of the system, expansion techniques such as those used by Merkin and Ingham,[9] were found to be numerically unstable when used to solve Eqs. (6) and (9). Therefore, whenever the shooting method becomes unstable, the continuation method as described by Bohl[10] has been employed.

The results for the centerline velocity, $V(0)$, are presented function of $\log_{10}|Ra_n|$ in Fig. 9 for $|Ra_n| < 10{,}000$. It can clearly be seen that for the Newtonian case, $n = 1$, that $V(0) \to \pm \infty$ at $Ra = Ra_c$, and that the value of each $|Ra_c|$ increases as the value of $n$ decreases, with the second value of $Ra_c$ being $-493.13$, $-503.81$, and $-554.95$ for $n = 1$, 0.9, and 0.8, respectively. A cycle can be defined as the continuous open curve between successive asymptotes, and then on each cycle the range of values of $Ra_n$ for which the multiple solution of $V(0)$ are $\mathcal{O}(1)$ increases in size as the value of $n$ decreases. As in the Newtonian case, the value of $V(0)$ can be either positive or negative, depending on the value of $Ra_n$. However, for certain values of $Ra_n$, when $n \neq 1$, one solution branch may have negative values of $V(0)$, while the other has positive values of $V(0)$. As the value of $n$ decreases, the gradient of the asymptotes that are defined by $V(0) \to \pm \infty$, decreases, i.e., for $Ra = Ra_c$, a given value of $V(0)$ on these curves

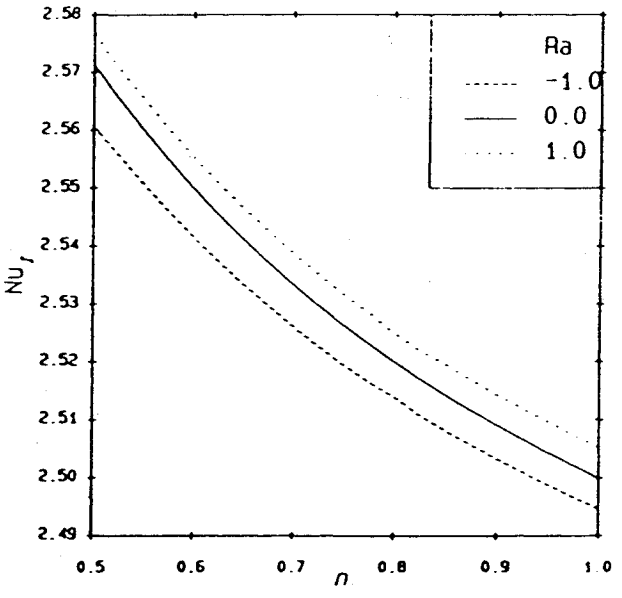


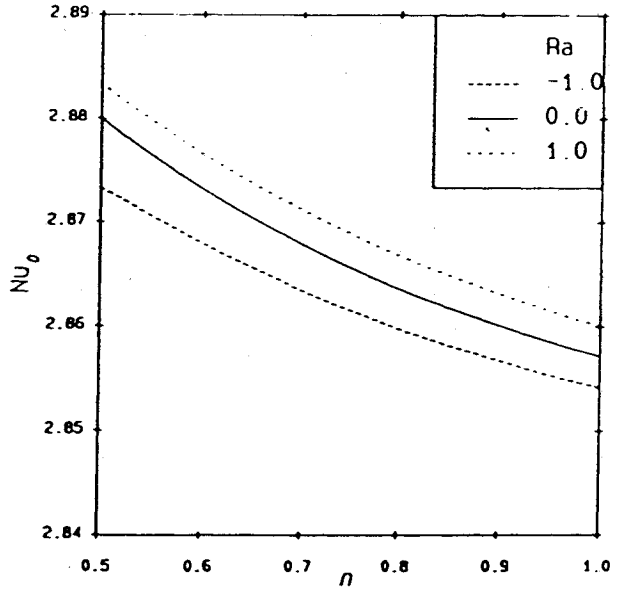


**Fig. 7 Nusselt numbers $Nu_f$ and $Nu_O$ for case II as functions of $n$ for $Ra_n = -1$, $Ra_n = 0$, and $Ra_n = 1$.**

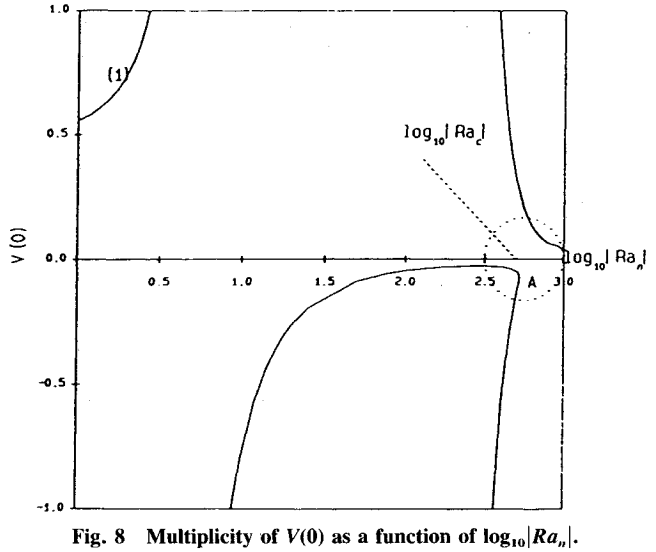


**Fig. 8 Multiplicity of $V(0)$ as a function of $\log_{10}|Ra_n|$.**

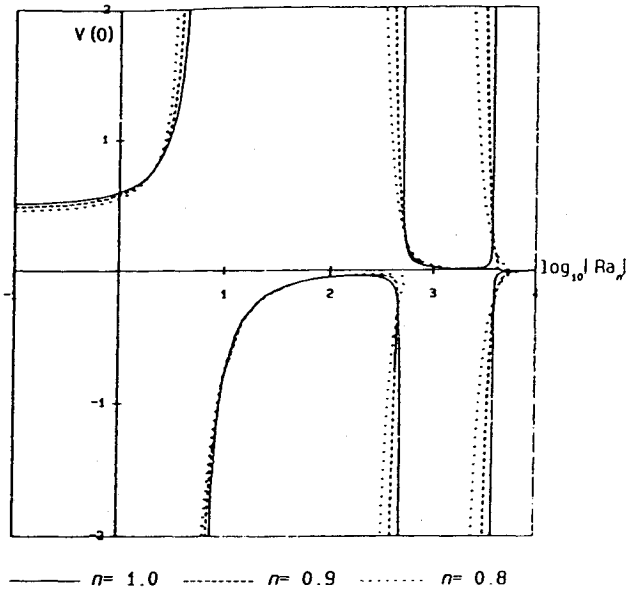


**Fig. 9 Centerline velocity $V(0)$ for case IA as a function of $\log_{10}|Ra_n|$ with $-10{,}000 < Ra_n < 0$, $n = 0.8$, 0.9, and 1.0, and $\zeta_n = 1.0$.**

occurs at smaller values of $Ra_n$ for lower values of $n$. This results from a flattening of the velocity profiles near the centerline of the duct as the value of $n$ decreases, and this is a common feature of power-law fluids. An important point to note is that the curve on the left side of each cycle has an obtuse-angled corner, while the turning point on the right side of the cycle has an acute-angled corner, although from the scale of Fig. 9 this is not obvious for the first value of $Ra_c$. The acute-angles on the $V(0)$ curve are the cause of the numerical instability that is encountered when trying to solve the governing equations using standard shooting methods.

## Discussion of Results

In this article, numerical investigations have been carried out into the fully developed flows of power-law fluids, and the results show good agreement with the limiting case of Newtonian flow. The velocity and buoyancy profiles for a power-law fluid depend on the direction of the flow and of the temperature gradient on the outer walls of the duct, unlike those in the corresponding Newtonian problem. The effects on the velocity and buoyancy force of varying both the Rayleigh number and parameters such as $\delta_2$ are discussed. The heat transfer increases as the value of the Rayleigh number increases, as in the Newtonian case, and increases as the value of the $n$ increases, as in the forced convection case.

It is of much mathematical interest to note that thermal runaway occurs for the flow of both Newtonian and power-law fluids when the wall temperature decreases with depth. Furthermore, it has been revealed that power-law fluids have multiple solutions for some ranges of values of the Rayleigh number. In order to obtain such solutions continuation methods have been used and novel results presented.

When the temperature increases with depth then the results presented in this paper are of much interest in the drilling and cementing of oil wells. The theory is applicable over almost the entire length of the piping and it is easy to extend to other non-Newtonian fluids, geometries, thermally varying properties, etc. At present there is very little experimental data, but when this becomes available the present theory will be invaluable in predicting the modifications to be made in the properties of the cement and muds being used in the oil industry to make these processes more efficient.

## Acknowledgments

The authors would like to thank Schlumberger Research for some financial support, and S. H. Bittleston for his valuable contribution to this project.

## References

[1]Kakac, S., Shah, R. K., and Aung, W., *Handbook of Single-Phase Convection Heat Transfer*, Wiley, New York, 1987.

[2]Ostrach, S., "Combined Natural and Forced Convection in Fluids with and Without Heat Sources in a Channel with Linearly Varying Wall Temperatures," NACA TN 3141, June 1954.

[3]Morton, B. R., "Laminar Convection in Uniformly Heated Vertical Pipes," *Journal of Fluid Mechanics*, Vol. 8, Pt. 2, 1960, pp. 227–240.

[4]Jackson, T. W., Harrison, W. B., and Boelter, W. C., "Combined Free and Forced Convection in a Vertical Tube," *Transactions of the American Society of Mechanical Engineers*, Vol. 80, Pt. 3, 1958, pp. 739–745.

[5]Hanratty, T. J., Rosen, E. M., and Kabel, R. L., "Effect of Heat Transfer on Flow Fields at Low Reynolds Number in Vertical Tubes," *Industrial and Engineering Chemistry*, Vol. 50, Pt. 3, 1958, pp. 815–820.

[6]Sherwin, K., "Laminar Convection in Uniformly Heated Vertical Concentric Annuli," *British Chemical Engineering*, Vol. 13, Pt. 3, 1968, pp. 569–574.

[7]Maitra, I. D., and Subba Raju, K., "Combined Free and Forced Convection Laminar Heat Transfer in a Vertical Annulus," *Journal of Heat Transfer*, Vol. 97, Pt. 1, 1960, pp. 135–137.

[8]Beckett, P. M., "Combined Natural and Forced Convection Between Parallel Vertical Walls," *SIAM Journal of Applied Maths*, Vol. 39, Pt. 2, 1980, pp. 372–384.

[9]Merkin, J. H., and Ingham, D. B., "Mixed Convection Similarity Solutions on a Horizontal Surface," *Journal of Applied Mathematics and Physics (ZAMP)*, Vol. 38, Pt. 1, 1987, pp. 102–116.

[10]Bohl, E., "Applications of Continuation Techniques in Ordinary Differential Equations," *The Numerical Solution of Non-Linear Problems*, edited by C. T. H. Baker and C. Phillips, Clarendon Press, Oxford, England, UK.